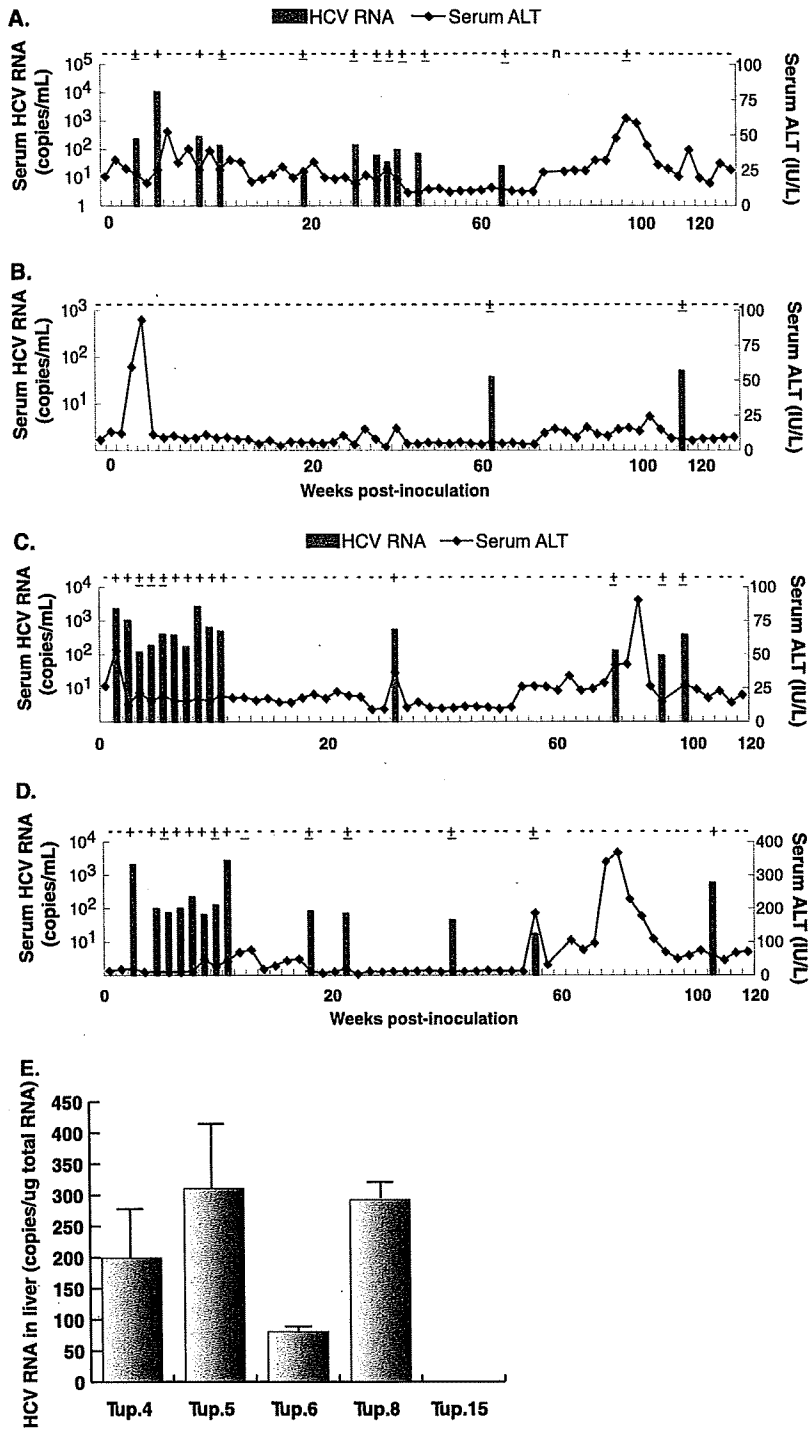

FIG. 1. Course of infection with patient serum HCR6 and RCV. (A) The results of quantitative RTD-PCR for HCV RNA and serum ALT concentrations were combined and plotted to show the course of infection in Tup.5. The bars and the ordinates on the left represent HCV RNA as genome equivalents/ml of serum. The curved line and the ordinates on the right represent serum ALT concentrations as IU/liter serum. (B) Serum HCV RNA and ALT concentrations for infection of Tup.6. (C) The graph for Tup.4. (D) The graph for Tup.8. The vertical axis for serum ALT in this graph is scaled differently from the others because of significant ALT elevation. (E) Quantification of HCV RNA in tupaia liver. HCV RNA in hepatocytes from tupaia (Tup.4, Tup.5, Tup.6, Tup.8, and Tup.15) livers was isolated 172 weeks after HCV infection and quantified by RTD-PCR. As few as 10 copies of the genome were detected, and the quantification range was between 10^1 and 10^8 copies (26).

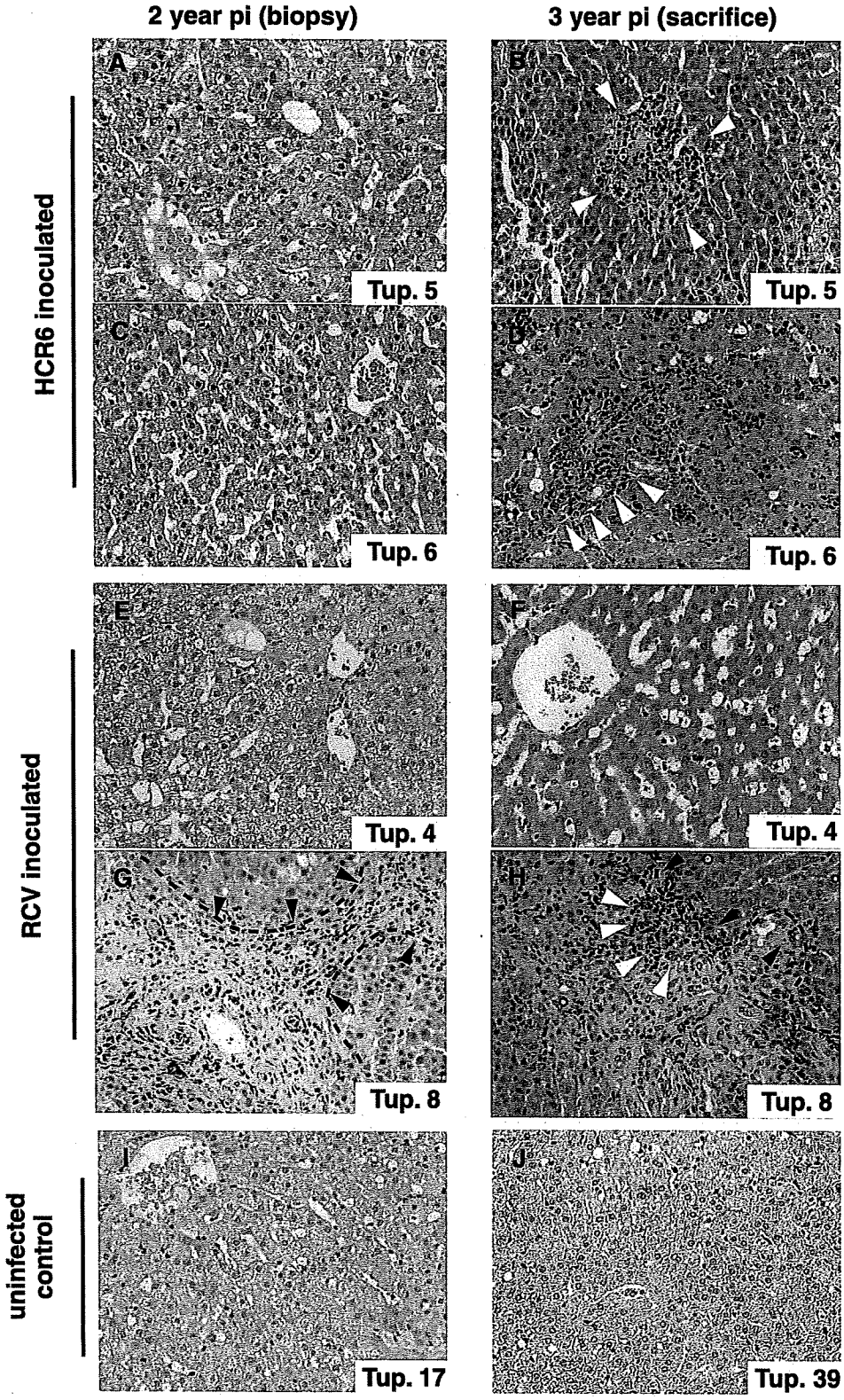

FIG. 2. Micrographs of liver specimens stained with H&E. Liver tissue from HCR6-inoculated tupaias (A to D) and RCV-inoculated tupaias (E to H) was obtained at 2 and 3 years postinoculation (pi). (I and J) Liver specimens from uninfected animals age matched to each inoculated animal were also obtained. The HCV-infected tupaia livers harbored infiltrating lymphocytes (white arrowheads) and fibrosis (broken lines and black arrowheads), which indicate chronic hepatitis.

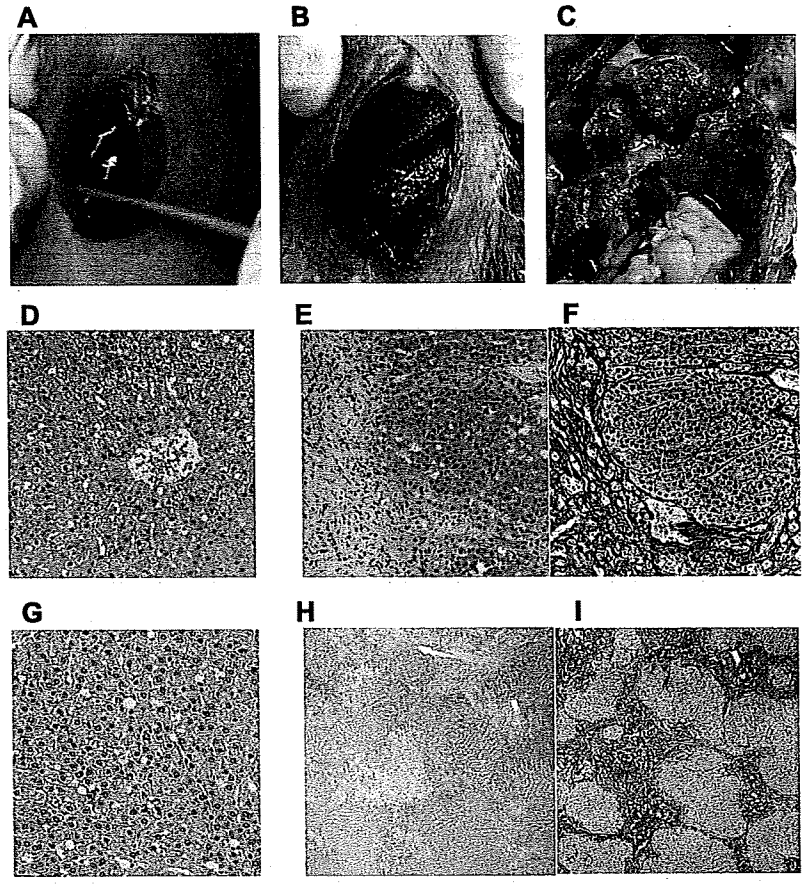

FIG. 3. Macro- and microscopic features of tupaia liver. (A) Infection-free control tupaia (Tup.15; 92 weeks). (B) RCV-infected animal displaying liver cirrhosis (Tup.8; 84 weeks postinoculation). (C) RCV-infected animal with massive surface nodules (Tup.8; 144 weeks postinoculation). (D and G) H&E staining of the uninfected Tup.15 at 92 weeks (D) and the uninfected Tup.39 at 242 weeks (G). (E, F, H, and I) H&E and silver staining of Tup.8 at 84 weeks postinoculation (E and F) or at 144 weeks postinoculation (H and I).

hepatitis had worsened with time in all HCV-infected tupaias (Fig. 2A to H and Table 2).

Fibrosis and cirrhosis were also examined. Mild fibrosis was seen in Tup.6, while severe fibrosis was seen in Tup.8. Cirrhosis was histologically investigated in all animals (Table 2). There was no significant difference between groups I and III at 94 weeks postinfection ($P = 0.194$), but at 144 weeks postinfection, a slight difference was observed ($P = 0.059$; SPSS 12.0). Macroscopic observation of the liver biopsy specimens (taken 2 years postinoculation) indicated liver cirrhosis in Tup.8 (Fig. 3B) compared with Tup.15 (uninfected control) (Fig. 3A), while silver staining of histology samples revealed fibrosis and cirrhotic nodules (Fig. 3E and F). Macroscopic observation upon sacrifice (3 years postinoculation) indicated that liver cirrhosis in Tup.8 had worsened (Fig. 3C). In contrast, age-matched infection-free negative control tupaias displayed none of these pathologies (Fig. 3A, D, and G).

Progressive lipid degeneration was noted in infected tupaias throughout the course of infection (Fig. 4). In particular, Tup.5 displayed microvesicular lipid droplets in the first biopsy specimens (at 2 years), which developed into macrovesicular droplets and foamy degeneration in biopsy specimens at 3 years (Fig. 4C and D). Liver specimens from other infected animals displayed intracellular micro- and macrovesicular lipid droplets in hepatocytes at 3 years postinoculation (Fig. 4F, H, and J). These anomalies were not present in liver specimens from infection-free control animals (Fig. 4A and B).

Transmission of viral-RNA-positive serum to naive animals reproduces acute hepatitis and viremia. To confirm virion regeneration in vivo, and to exclude the possibility of false-positive serum HCV RNA results due to amplification of the original inocula, HCV RNA-positive sera from primary inoculated tupaias were used to inoculate naive tupaias. Three different sera were tested in this passage experiment, with two naive tupaias used as recipient animals for each trial (see Materials and Methods) (Table 1, group II).

In the first reinfection experiment, serum from Tup.5 (originally infected with patient serum HCR6) was collected at 5 weeks postinoculation and used to infect two naive animals. The recipient animals showed intermittent viremia over the subsequent 3 months (Fig. 5A). In the second and third cases of reinfection, sera from Tup.8 at 10 weeks postinoculation and from Tup.4 at 8 weeks postinoculation also induced viremia in the naive inoculated animals, similar to the first reinfection experiment (Fig. 5B and C). Furthermore, the PCR titers of the recipient tupaias were significantly greater than the inoc-

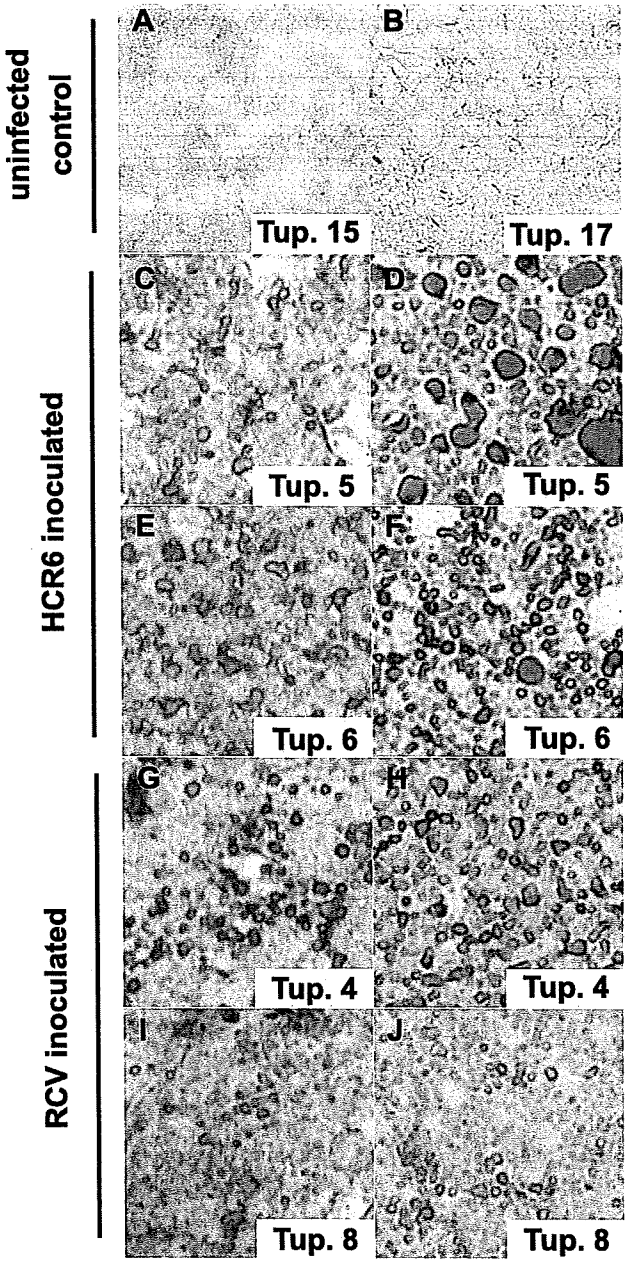

FIG. 4. Sudan IV-stained liver specimens exhibiting fatty liver degeneration. Cryosections of liver stained by Sudan IV as described in Materials and Methods show fatty liver degeneration. The left and right columns display biopsy specimens of infected animals (2 years postinoculation) and animals sacrificed at 3 years postinfection, respectively. (A and B) Uninfected controls at 2 years (Table 1 shows sample timing). (C to F) Patient serum HCR6-infected animals. (G to J) RCV-infected animals.

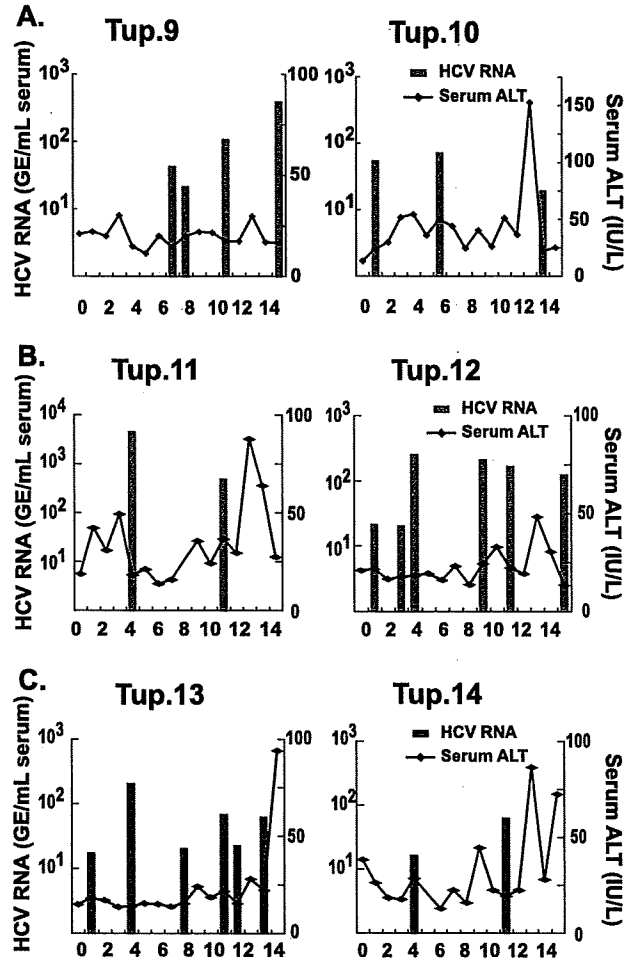

FIG. 5. Results of a reinfection experiment. (A) Quantitative RTD-PCR for HCV RNA and serum ALT levels are shown. Two naive animals were inoculated with tupaia serum (using serum taken at 5 weeks postinoculation from Tup.5, originally inoculated with patient serum HCR6) containing 100 genome equivalents (GE)/ml and were monitored for 15 weeks postinoculation (Table 1). (B) Tupaia serum (taken at 10 weeks postinoculation from Tup.8, originally inoculated with RCV) that was positive for HCV RNA was passaged into two naive animals. The animals were inoculated with tupaia serum at 100 GE/animal and monitored for 15 weeks postinoculation. (C) Tupaia serum (taken at 8 weeks postinoculation from Tup.4, originally inoculated with RCV) that was positive for HCV RNA was passaged into naive animals. The animals were inoculated with serum at 100 GE/animal and monitored for 20 weeks postinoculation.

ulation titers (10^2 genome equivalents/animal) (Table 1). For Tup.11, serum from 4 weeks postinoculation contained almost 10^4 genome equivalents/ml of HCV RNA (Fig. 5B). In addition, significant increases in serum ALT accompanied detection of serum HCV RNA. These results indicate that HCV RNA-positive sera from group I actually contained infectious virion particles. They also suggest that reconstituted HCV particles made from cDNA are infectious in tupaias.

We amplified a portion of the NS5A sequence, which is known as the interferon sensitivity determining region, by reverse transcription-PCR as described in the supplemental material. Each PCR product was subcloned and sequenced to compare the encoded amino acid sequences. For the purposes of this study, animals were inoculated with a molecular clonal virus consisting of a unique viral sequence of cDNA. The interferon sensitivity determining region sequences recovered from an animal infected with clonal inoculum (Tup.8 at 103 weeks postinoculation) were found to be heterogeneous, with

a few amino acid substitutions (K2212M for 2/10 cases, L2232P for 1/10 cases, and L2253S for 6/10 cases) (see Fig. S2E in the supplemental material). Interestingly, the codon for amino acid 2224 encodes valine, but it was found to be variant for alanine and valine in sequences from the original patient serum (HCR6). Tupaias infected with patient serum also exhibited variability at position 2224; valine occupancy was rare, as was seen in the original HCR6 population (see Fig. S2B and C in the supplemental material). On the other hand, this position was occupied solely by valine for sequences recovered from Tup.8 (see Fig. S2E in the supplemental material), indicating that genetic variations shown for Tup.8 originated from the pHCR6 cDNA sequence. Taken together, quasispecies detection of circulating virus represents further evidence demonstrating intrinsic replication of HCV in tupaias despite low levels and infrequent detection of viremia.

DISCUSSION

In the present study, we described persistent HCV infection in tupaias. Long-term follow-up was performed and revealed histological progression of HCV-related liver disorders in infected tupaias, including steatosis, fibrosis, and cirrhosis, in addition to acute and chronic hepatitis. HCV genomic RNA was detected in animal sera intermittently throughout the entire course of infection. However, HCV RNA was detected in the liver upon sacrifice (3 years postinoculation). Furthermore, HCV RNA in serum contained genomic variants that had diverged from the inoculated virus (see Fig. S1 and S2 in the supplemental material). These data strongly indicate an established persistent infection in the tupaias studied. All animals exhibited HCV viremia soon after inoculation, yet the viremia was intermittent and accompanied by relatively low RTD-PCR titers compared with equivalent human and chimpanzee infections. The discrepancy between humans and tupaias might be due to host-dependent differences in replication efficiency. Over the course of HCV infection in these tupaias, serum ALT profiles indicated repeated liver injury, probably due to host immune responses mediated by agents such as cytotoxic T lymphocytes rather than direct viral cytopathic effects.

In cases of tupaia infection, experimental inoculations rarely led to sustained viremia, which for most human cases lasts for the entire course of infection. Even the course of infection appeared transient and self-resolved. It seems likely that HCV replication is less compatible with the tupaia host environment. This possibility was substantiated by a previous report by Xu et al. (34), where tissue-cultured virions of cloned genotype 1b, referred to as HCVcc in the paper, could not cause chronic infection with sustained viremia in tupaias. Although HCVcc actually infected most of the inoculated tupaias (83%; 10/12), chronic infection was seen for only a fraction of them (20%; 2/10). In this study, we also tried to detect a humoral response to HCV core antigen. We found that tupaia sera were HCV positive for antibodies only at occasional time points, observable as intermittent steep responses (data not shown). Overall, sustained seroconversion was not seen in this study, probably because HCV propagation in vivo was so limited or well controlled by host immunity. Given that models of HCV propagation are severely limited, the most important and interesting finding of this study is the successful detection of HCV RNA in livers of infected tupaias 3 years after inoculation, indicating that HCV persists in tupaias. Although the limited propagation of HCV in tupaias is a drawback of this model at the present time, the isolation of tupaia-adapted HCV may be feasible by performing multiple infection passages. This possibility is supported by both quasispecies development and successful reinfection.

The chimpanzee is the animal species most closely related to humans, and as a model, it has contributed significantly to our understanding of HCV infection and pathogenesis. However, reproducing HCV pathogenesis in humans or chimpanzees can take as long as 10 to 20 years. The chronically infected tupaias in the present study developed complicated liver disorders in a much shorter time. Using tupaias, with their relatively short life span (3 to 5 years in the laboratory), as a model of HCV infection, we can evaluate HCV pathogenesis and correlate senescence and duration of infection.

The recent development of a primary human hepatocyte xenograft-uPA/SCID mouse model opened up opportunities to test putative antivirals against HCV replication in vivo (10, 17). In this innovative model, human hepatocytes, which are transplanted into the lobe of a mouse liver, can support HCV replication effectively. As a result, the level of circulating HCV RNA is comparable to that of a human patient. However, this mouse model is immunodeficient, and thus, it lacks the interplay between host immunity and viral infection. Therefore, it does not provide a suitable platform for characterizing immune responses to HCV infection.

HCV infection in tupaias represents an important model of HCV infection, particularly for the study of key determinants controlling virus propagation in vivo. The pathogenesis of HCV infection can be substantially different among humans, chimpanzees, and tupaias, and the mechanisms governing these differences are of great interest. Comparative studies of HCV infection in these different species will help us to understand the basic mechanisms of persistent infection.

ACKNOWLEDGMENTS

We thank Masahiro Shuda for helpful assistance and Etsuko Endo for creating the figures. We also thank the staffs of the Departments of Microbiology and Cell Biology and Mitsugu Takahashi for breeding the tupaias.

This study was supported by grants from the Ministry of Education, Culture, Sports, Science and Technology of Japan; the Program for Promotion of Fundamental Studies in Health Sciences of the Pharmaceuticals and Medical Devices Agency of Japan; and the Ministry of Health, Labor and Welfare of Japan.

REFERENCES

1. **Abe, K., T. Kurata, Y. Teramoto, J. Shiga, and T. Shikata.** 1993. Lack of susceptibility of various primates and woodchucks to hepatitis C virus. J. Med. Primatol. **22**:433–434.
2. **Aoki, Y., H. Aizaki, T. Shimoike, H. Tani, K. Ishii, I. Saito, Y. Matsuura, and T. Miyamura.** 1998. A human liver cell line exhibits efficient translation of HCV RNAs produced by a recombinant adenovirus expressing T7 RNA polymerase. Virology **250**:140–150.
3. **Chomczynski, P., and N. Sacchi.** 1987. Single-step method of RNA isolation by acid guanidinium thiocyanate-phenol-chloroform extraction. Anal. Biochem. **162**:156–159.
4. **Choo, Q. L., G. Kuo, A. J. Weiner, L. R. Overby, D. W. Bradley, and M. Houghton.** 1989. Isolation of a cDNA clone derived from a blood-borne non-A, non-B viral hepatitis genome. Science **244**:359–362.
5. **Dash, S., G. Kalkeri, H. M. McClure, R. F. Garry, S. Clejan, S. N. Thung, and K. K. Murthy.** 2001. Transmission of HCV to a chimpanzee using virus

particles produced in an RNA-transfected HepG2 cell culture. J. Med. Virol. **65**:276–281.
6. **Flugge, P., E. Fuchs, E. Gunther, and L. Walter.** 2002. MHC class I genes of the tree shrew Tupaia belangeri. Immunogenetics **53**:984–988.
7. **Goldsmith, E. I.** 1978. The convention on international trade in endangered species of wild fauna and flora. J. Med. Primatol. **7**:122–124.
8. **Hong, Z., M. Beaudet-Miller, R. E. Lanford, B. Guerra, J. Wright-Minogue, A. Skelton, B. M. Baroudy, G. R. Reyes, and J. Y. Lau.** 1999. Generation of transmissible hepatitis C virions from a molecular clone in chimpanzees. Virology **256**:36–44.
9. **Hoofnagle, J. H.** 2002. Course and outcome of hepatitis C. Hepatology **36**:S21–S29.
10. **Inoue, K., T. Umehara, U. T. Ruegg, F. Yasui, T. Watanabe, H. Yasuda, J. M. Dumont, P. Scalfaro, M. Yoshiba, and M. Kohara.** 2007. Evaluation of a cyclophilin inhibitor in hepatitis C virus-infected chimeric mice in vivo. Hepatology **45**:921–928.
11. **Ishak, K., A. Baptista, L. Bianchi, F. Callea, J. De Groote, F. Gudat, H. Denk, V. Desmet, G. Korb, R. N. MacSween, et al.** 1995. Histological grading and staging of chronic hepatitis. J. Hepatol. **22**:696–699.
12. **Ito, T., K. Yasui, J. Mukaigawa, A. Katsume, M. Kohara, and K. Mitamura.** 2001. Acquisition of susceptibility to hepatitis C virus replication in HepG2 cells by fusion with primary human hepatocytes: establishment of a quantitative assay for hepatitis C virus infectivity in a cell culture system. Hepatology **34**:566–572.
13. **Kock, J., M. Nassal, S. MacNelly, T. F. Baumert, H. E. Blum, and F. von Weizsacker.** 2001. Efficient infection of primary tupaia hepatocytes with purified human and woolly monkey hepatitis B virus. J. Virol. **75**:5084–5089.
14. **Kolykhalov, A. A., E. V. Agapov, K. J. Blight, K. Mihalik, S. M. Feinstone, and C. M. Rice.** 1997. Transmission of hepatitis C by intrahepatic inoculation with transcribed RNA. Science **277**:570–574.
15. **Major, M. E., and S. M. Feinstone.** 1997. The molecular virology of hepatitis C. Hepatology **25**:1527–1538.
16. **Marcellin, P., T. Asselah, and N. Boyer.** 2002. Fibrosis and disease progression in hepatitis C. Hepatology **36**:S47–S56.
17. **Mercer, D. F., D. E. Schiller, J. F. Elliott, D. N. Douglas, C. Hao, A. Rinfret, W. R. Addison, K. P. Fischer, T. A. Churchill, J. R. Lakey, D. L. Tyrrell, and N. M. Kneteman.** 2001. Hepatitis C virus replication in mice with chimeric human livers. Nat. Med. **7**:927–933.
18. **Nascimbeni, M., E. Mizukoshi, M. Bosmann, M. E. Major, K. Mihalik, C. M. Rice, S. M. Feinstone, and B. Rehermann.** 2003. Kinetics of CD4+ and CD8+ memory T-cell responses during hepatitis C virus rechallenge of previously recovered chimpanzees. J. Virol. **77**:4781–4793.
19. **Pawlotsky, J. M.** 2002. Use and interpretation of virological tests for hepatitis C. Hepatology **36**:S65–S73.
20. **Ren, S., and M. Nassal.** 2001. Hepatitis B virus (HBV) virion and covalently closed circular DNA formation in primary tupaia hepatocytes and human hepatoma cell lines upon HBV genome transduction with replication-defective adenovirus vectors. J. Virol. **75**:1104–1116.
21. **Seeff, L. B.** 2002. Natural history of chronic hepatitis C. Hepatology **36**:S35–S46.
22. **Shimayama, T., S. Nishikawa, and K. Taira.** 1995. Generality of the NUX rule: kinetic analysis of the results of systematic mutations in the trinucleotide at the cleavage site of hammerhead ribozymes. Biochemistry **34**:3649–3654.
23. **Shimizu, Y. K., H. Igarashi, T. Kanematu, K. Fujiwara, D. C. Wong, R. H. Purcell, and H. Yoshikura.** 1997. Sequence analysis of the hepatitis C virus genome recovered from serum, liver, and peripheral blood mononuclear cells of infected chimpanzees. J. Virol. **71**:5769–5773.
24. **Shimizu, Y. K., A. Iwamoto, M. Hijikata, R. H. Purcell, and H. Yoshikura.** 1992. Evidence for in vitro replication of hepatitis C virus genome in a human T-cell line. Proc. Natl. Acad. Sci. USA **89**:5477–5481.
25. **Suh, Y. A., P. K. Kumar, K. Taira, and S. Nishikawa.** 1993. Self-cleavage activity of the genomic HDV ribozyme in the presence of various divalent metal ions. Nucleic Acids Res. **21**:3277–3280.
26. **Takeuchi, T., A. Katsume, T. Tanaka, A. Abe, K. Inoue, K. Tsukiyama-Kohara, R. Kawaguchi, S. Tanaka, and M. Kohara.** 1999. Real-time detection system for quantification of hepatitis C virus genome. Gastroenterology **116**:636–642.
27. **Tanaka, T., N. Kato, M. J. Cho, K. Sugiyama, and K. Shimotohno.** 1996. Structure of the 3′ terminus of the hepatitis C virus genome. J. Virol. **70**:3307–3312.
28. **Thomson, M., M. Nascimbeni, M. B. Havert, M. Major, S. Gonzales, H. Alter, S. M. Feinstone, K. K. Murthy, B. Rehermann, and T. J. Liang.** 2003. The clearance of hepatitis C virus infection in chimpanzees may not necessarily correlate with the appearance of acquired immunity. J. Virol. **77**:862–870.
29. **Tsukiyama-Kohara, K., N. Iizuka, M. Kohara, and A. Nomoto.** 1992. Internal ribosome entry site within hepatitis C virus RNA. J. Virol. **66**:1476–1483.
30. **Tsukiyama-Kohara, K., S. Tone, I. Maruyama, K. Inoue, A. Katsume, H. Nuriya, H. Ohmori, J. Ohkawa, K. Taira, Y. Hoshikawa, F. Shibasaki, M. Reth, Y. Minatogawa, and M. Kohara.** 2004. Activation of the CKI-CDK-Rb-E2F pathway in full genome hepatitis C virus-expressing cells. J. Biol. Chem. **279**:14531–14541.
31. **Walter, E., R. Keist, B. Niederost, I. Pult, and H. E. Blum.** 1996. Hepatitis B virus infection of tupaia hepatocytes in vitro and in vivo. Hepatology **24**:1–5.
32. **Wasley, A., and M. J. Alter.** 2000. Epidemiology of hepatitis C: geographic differences and temporal trends. Semin. Liver Dis. **20**:1–16.
33. **Xie, Z. C., J. I. Riezu-Boj, J. J. Lasarte, J. Guillen, J. H. Su, M. P. Civeira, and J. Prieto.** 1998. Transmission of hepatitis C virus infection to tree shrews. Virology **244**:513–520.
34. **Xu, X., H. Chen, X. Cao, and K. Ben.** 2007. Efficient infection of tree shrew (Tupaia belangeri) with hepatitis C virus grown in cell culture or from patient plasma. J. Gen. Virol. **88**:2504–2512.
35. **Yanagi, M., R. H. Purcell, S. U. Emerson, and J. Bukh.** 1997. Transcripts from a single full-length cDNA clone of hepatitis C virus are infectious when directly transfected into the liver of a chimpanzee. Proc. Natl. Acad. Sci. USA **94**:8738–8743.
36. **Yanagi, M., M. St Claire, M. Shapiro, S. U. Emerson, R. H. Purcell, and J. Bukh.** 1998. Transcripts of a chimeric cDNA clone of hepatitis C virus genotype 1b are infectious in vivo. Virology **244**:161–172.
37. **Zhao, X., Z. Y. Tang, B. Klumpp, G. Wolff-Vorbeck, H. Barth, S. Levy, F. von Weizsacker, H. E. Blum, and T. F. Baumert.** 2002. Primary hepatocytes of Tupaia belangeri as a potential model for hepatitis C virus infection. J. Clin. Invest. **109**:221–232.

GASTROENTEROLOGY 2009;137:285–296

BASIC—LIVER, PANCREAS, AND BILIARY TRACT

Hepatitis C Virus and Disrupted Interferon Signaling Promote Lymphoproliferation via Type II CD95 and Interleukins

KEIGO MACHIDA,[*,‡,§] KYOKO TSUKIYAMA-KOHARA,[*,‖] SATOSHI SEKIGUCH,[*] EIJI SEIKE,[¶] SHIGENOBU TÓNE,[#] YUKIKO HAYASHI,[**] YOSHIMI TOBITA,[*] YURI KASAMA,[‖] MASUMI SHIMIZU,[‡‡] HIDEMI TAKAHASHI,[‡‡] CHYOJI TAYA,[§§] HIROMICHI YONEKAWA,[§§] NOBUYUKI TANAKA,[‡,‖‖] and MICHINORI KOHARA[*]

[*]*Department of Microbiology and Cell Biology, Tokyo Metropolitan Institute of Medical Science, Tokyo, Japan;* [‡]*Department of Immunology, Graduate School of Medicine and Faculty of Medicine, University of Tokyo, Tokyo, Japan;* [§]*Department of Molecular Microbiology and Immunology, Keck School of Medicine, University of Southern California, Los Angeles, California;* [‖]*Department of Experimental Phylaxiology, Faculty of Medical and Pharmaceutical Sciences, Kumamoto University, Kumamoto, Japan;* [¶]*Department of Internal Medicine, Self-Defense Forces Central Hospital, Tokyo, Japan;* [#]*Department of Biochemistry, Kawasaki Medical School, Okayama, Japan;* [**]*Department of Pathology, Tokyo Metropolitan Komagome Hospital, Tokyo, Japan;* [‡‡]*Department of Microbiology and Immunology, Nippon Medical School, Tokyo, Japan;* [§§]*Laboratory of Animal Science, Tokyo Metropolitan Institute of Medical Science, Tokyo, Japan; and* [‖‖]*Department of Molecular Oncology, Institute of Gerontology, Nippon Medical School, Kanagawa, Japan*

BACKGROUND & AIMS: The molecular mechanisms of lymphoproliferation associated with the disruption of interferon (IFN) signaling and chronic hepatitis C virus (HCV) infection are poorly understood. Lymphomas are extrahepatic manifestations of HCV infection; we sought to clarify the molecular mechanisms of these processes. **METHODS:** We established interferon regulatory factor-1–null (irf-1$^{-/-}$) mice with inducible and persistent expression of HCV structural proteins (irf-1/CN2 mice). All the mice (n = 900) were observed for at least 600 days after Cre/loxP switching. Histologic analyses, as well as analyses of lymphoproliferation, sensitivity to Fas-induced apoptosis, colony formation, and cytokine production, were performed. Proteins associated with these processes were also assessed. **RESULTS:** *Irf-1*/CN2 mice had extremely high incidences of lymphomas and lymphoproliferative disorders and displayed increased mortality. Disruption of *irf-1* reduced the sensitivity to Fas-induced apoptosis and decreased the levels of caspases-3/7 and caspase-9 messenger RNA species and enzymatic activities. Furthermore, the *irf-1*/CN2 mice showed decreased activation of caspases-3/7 and caspase-9 and increased levels of interleukin (IL)-2, IL-10, and Bcl-2, as well as increased Bcl-2 expression, which promoted oncogenic transformation of lymphocytes. IL-2 and IL-10 were induced by the HCV core protein in splenocytes. **CONCLUSIONS: Disruption of IFN signaling resulted in development of lymphoma, indicating that differential signaling occurs in lymphocytes compared with liver. This mouse model, in which HCV expression and disruption of IFN signaling synergize to promote lymphoproliferation, will be an important tool for the development of therapeutic agents that target the lymphoproliferative pathway.**

More than 175 million people worldwide are infected with hepatitis C virus (HCV), which is a positive-strand RNA virus that infects both hepatocytes and peripheral blood mononuclear cells.[1–4] Chronic hepatitis infection can lead to hepatitis, cirrhosis, hepatocellular carcinoma, and lymphoproliferative diseases, such as B-cell non-Hodgkin's lymphomas and mixed cryoglobulinemia.[5–10] The current therapy for chronic HCV infection involves treatment with type I interferon (IFN) and derivatives of IFN, such as pegylated IFN.[11] Treatment with type I IFN is associated with regression of lymphoma in patients with hepatitis C.[12] However, more than 50% of HCV-infected individuals are resistant to treatment, which indicates that the inhibition of IFN signal transduction facilitates the persistent expression of HCV proteins by hepatocytes.

Transgenic mice that express the HCV core protein have been established using a promoter derived from hepatitis B virus,[13] whereas mice that express structural or complete viral proteins have been established using promoters derived from the albumin gene.[14] These mice are immunotolerant to the transgene and do not develop hepatic inflammation, although they do develop age-related hepatic steatosis and hepatocellular carcinomas. We also developed a transgenic mouse model in which the HCV complementary DNA, including viral genes that encode the core, E1, E2, and NS2 proteins, was conditionally expressed by the Cre/*lox*P system (CN2 mice).[15]

Abbreviations used in this paper: IFN, interferon; IL, interleukin; IRF, interferon-regulatory factor; PCR, polymerase chain reaction; WT, wild-type.

0016-5085/09/$36.00
doi:10.1053/j.gastro.2009.03.061

The conditional expression of HCV proteins protected mice from Fas-mediated lethal acute liver failure by inhibiting cytochrome *c* release from the mitochondria.[16] However, the expression of HCV in these mice was usually lost after 21 days. Therefore, an animal model of persistent HCV protein expression is required to examine the effects of chronic HCV infection in vivo.

IFN signaling mediates tumor suppressor effects and antiviral responses and is regulated by key transcription factors of the interferon-regulatory factor (IRF) protein family, including Irf-1, -2, -3, -7, and -9. Targeted disruption of *irf-1* results in aberrant lymphocyte development and a marked reduction in the number of $CD8^+$ T cells in the peripheral blood, spleen, and lymph nodes.[17] In addition, natural killer cell development is impaired in *irf-1*$^{-/-}$ mice.[18] The mechanisms by which HCV infection induces IFN resistance and influences the development of lymphomas are poorly understood. Therefore, in the present study, we established an *irf-1*$^{-/-}$ CN2 mouse model of persistent HCV expression, which allows investigation of the effects of HCV on lymphatic tissue tumor development.

Materials and Methods

Animal Experiments

Wild-type (WT), CN2, *irf-1*$^{-/-}$, and *Mx1-cre* mice were maintained in conventional animal housing under specific pathogen-free conditions. AxCANCre and AxCAw1 were obtained from Dr Izumu Saito (University of Tokyo).[15] To elicit Fas-induced liver damage, adult mice were injected intravenously with 10 μg of purified hamster monoclonal antibody against mouse Fas (clone Jo2; BD Biosciences, San Diego, CA) in 200 μL of phosphate-buffered saline. All animal experiments were performed according to the guidelines of the Tokyo Metropolitan Institute of Medical Science or Kumamoto University Subcommittee for Laboratory Animal Care. The protocol was approved by an institutional review board. Detailed procedures, including induction of the HCV transgene by poly(I:C) in CN2-29 Mx1-Cre mice, are described in Supplementary Materials and Methods.

Measurements of Caspase Activities

The cytosolic splenocyte fractions were isolated as described,[16] and the detailed procedures are described in the Supplementary Material and Methods.

Lentiviral Vectors and Infection

Isolated splenocytes from WT or *irf-1*$^{-/-}$ mice (total of 10^7 cells) were infected with recombinant lentiviruses that express HCV core, E1, E2, NS2, *lacZ*, and empty vector, respectively. One day after infection, cells were selected with puromycin (final concentration of 1 μg/mL). After 5 days of puromycin selection, viable cells were examined.

Baculovirus Expression and Purification of HCV Core, E1, and E2 Proteins

The E1 and E2 sequences from a genotype 1a isolate (strain H77)[19] and a genotype 1b isolate (strain HC-J4),[20] without the C-terminal transmembrane domains but containing the His_6 tag at the C terminus, were cloned into a transfer vector (pBlueBacHis2; Invitrogen, Carlsbad, CA). The expression of recombinant core, E1, and E2 proteins in insect cells and their purification have been described previously.[21]

Results

Viral Protein Expression and Disruption of irf-1 *Synergistically Increase the Development of Lymphoproliferative Disorders*

To clarify the in vivo effects of HCV protein expression, we examined the survival of mice that carry the CN2 transgene (CN2-8, CN2-29).[15] The experimental design is shown in Figure 1*A* (total number of mice, 900). Without Cre/*lox*P switching, the animals that carry the HCV transgene (CN2-8 and CN2-29: core, E1, E2, and NS2 proteins) appeared healthy and developed normally.[15] All of the transgene carriers were observed for at least 600 days after Cre/*lox*P switching (Figure 1*A*). Administration of a recombinant adenovirus that expresses *cre* (AxCANCre) induced the efficient recombination of CN2 transgenes in the hepatocytes from CN2 and *irf-1*$^{-/-}$ CN2 mice (Figure 1*B*). Recombination produced the floxed CN2 transgene (3.3 kilobases) and was completed within 4–7 days; it diminished before day 21 in CN2 mice but persisted in *irf-1*$^{-/-}$ CN2 mice. The expression of core protein in the hepatocytes of CN2 mice peaked on day 7 and decreased to an undetectable level by day 21 (Supplementary Figure 1*A*). The expression of core protein in hepatocytes coincided with a high level of inflammation, as determined by measurements of serum alanine aminotransferase activity (Supplementary Figure 1*A* and data not shown). The HCV core protein was detected in CN2-8 mice 4–14 days after the administration of AxCANCre, and disruption of *irf-1* ensured core protein expression for more than 500 days (Supplementary Figure 1*A* and 1*B*). Therefore, *irf-1* disruption allowed efficient and persistent expression of HCV proteins. HCV core protein gene expression was confirmed by reverse-transcription polymerase chain reaction (PCR) of livers, splenocytes, and peripheral blood monocytes (Supplementary Figure 1*C*). AxCANCre administration to the transgenic mouse induced the efficient expression of HCV transgenes in lymphocytes and splenocytes (Supplementary Figure 1*C*).

The survival rate of WT mice injected with the *cre*-adenovirus (AxCANCre) (Figure 1*C*) or control adenovirus (AxCAw1) (data not shown) was higher than that of the transgenic mice (CN2-8 and CN2-29), which excludes the possibility that the recombinant adenovirus affec-

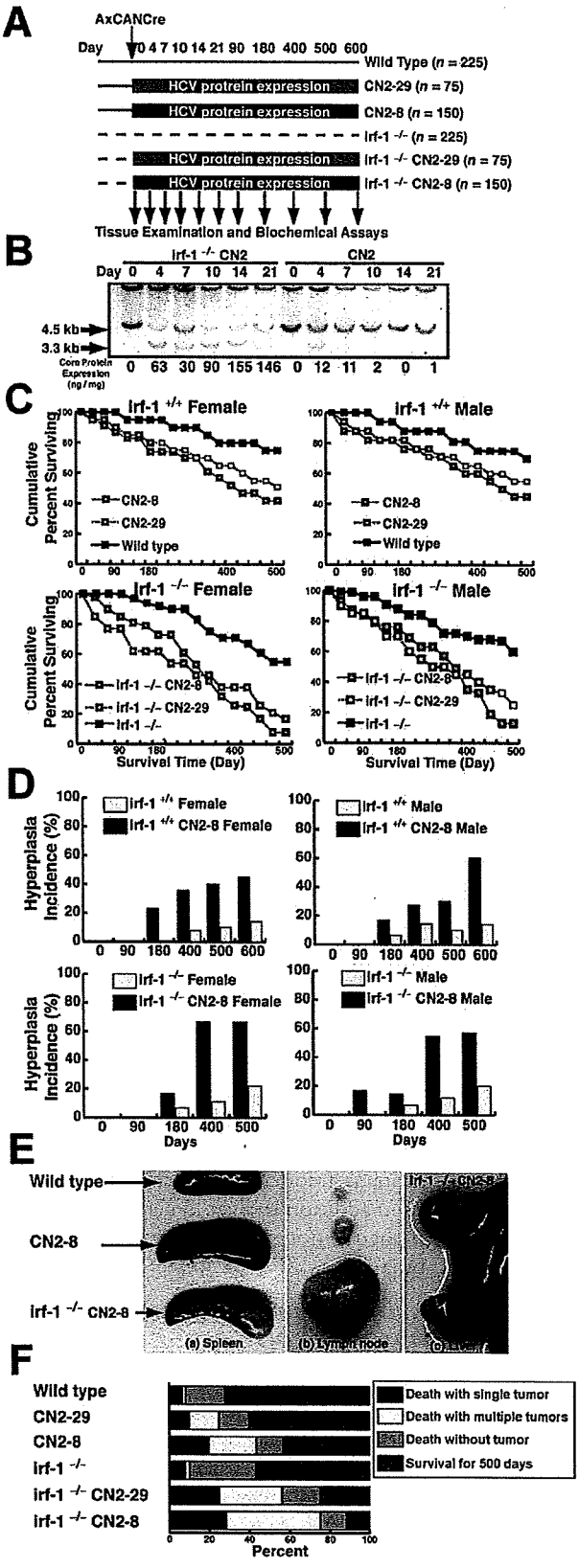

ted the results. More than 75% of the WT mice injected with AxCANCre survived to day 500, whereas the HCV-expressing mice had lower survival rates. The *irf-1*$^{-/-}$ CN2-8 and *irf-1*$^{-/-}$ CN2-29 strains had even lower survival rates, indicating that persistent HCV protein expression in combination with *irf-1* disruption significantly decreases survival (Figure 1*C*).

Lymphoproliferative Disorders Are Accelerated With Age and Level of Viral Protein Expression

To determine the mechanism underlying the increased mortality caused by persistent HCV protein expression in *irf-1*$^{-/-}$ CN2 mice, we examined the kinetics of dysplasia (Figure 1*D*). Strikingly, 67% of the female *irf-1*$^{-/-}$ CN2 mice and 70% of the male *irf-1*$^{-/-}$ CN2 mice developed tumors 400 days after the administration of AxCANCre. Some of the *irf-1*$^{-/-}$ CN2 mice developed hyperplasia of the lymph nodes, and these tumors developed much earlier than the tumors in their *irf-1*$^{+/+}$ or CN2 counterparts (Figure 1*D*). Aberrant cell proliferation developed randomly among the male and female carrier animals between day 180 and day 600. On day 400 after Cre/*lox*P switching, the average weights of the spleens of the WT, CN2, and *irf-1*$^{-/-}$ CN2 mice were 90, 160, and 310 mg, respectively. The disruption of *irf-1* aggravated the HCV-induced spontaneous proliferative disturbances in lymphatic tissues. The number of CN2 mice that died with at least one tumor and the number of tumors per

Figure 1. Disruption of *irf-1* enhances oncogenic potential in combination with HCV transgene expression. (*A*) Experimental design for the animal model. Transgenic mice and their nontransgenic littermates (10–14 weeks of age) were administered the *Cre*-expressing adenovirus (AxCANCre) and killed after 4, 7, 10, 14, 21, 90, 120, 400, 500, or 600 days. (*B*) Southern blot analysis of hepatocyte DNA from mice derived by crossing *irf-1*$^{-/-}$ and HCV-transgenic (CN2) mice. Genomic DNA samples from WT (+/+) and CN2 mouse hepatocytes were digested with *Xba*I and subjected to Southern blot analysis using a radiolabeled genomic flanking probe to determine the rate of recombination of the HCV transgene construct (3.3-kilobase fragment). Disruption of *irf-1* allows persistent expression of HCV proteins. The effects of HCV protein expression on the survival rates of male and female *irf-1*$^{-/-}$ and *irf-1*$^{+/+}$ CN2 mice are shown. (*C*) Kaplan–Meier survival curves for WT mice, *irf-1*$^{-/-}$ mice, CN2 transgenic mouse strains 8 and 29, and *irf-1*$^{-/-}$ CN2-8 and CN-29 mice following infection with a recombinant adenovirus that expresses *cre* (AxCANCre). (*D*) HCV protein expression enhances hyperplasia in male and female CN2 and *irf-1*$^{-/-}$ CN2 mice. The occurrence of hyperplasia was monitored every 7 days for 600 days following the administration of AxCANCre. (*E*) Spleens (*a*) and lymph nodes (*b*) from age-matched WT, CN2, and *irf-1*$^{-/-}$ CN2 mice 500 days after the administration of AxCANCre. (*c*) Liver from the same *irf-1*$^{-/-}$ CN2 mouse (developing severe lymphadenopathy and splenomegaly) following the administration of AxCANCre. (*F*) The cause of death in CN2 transgenic mice with hyperplasias. Mice of each genotype (n = 150) were monitored up to day 600 after the administration of AxCANCre, and necropsies were performed to determine the number of tumors. Tumors included thymomas, splenomas, lymphomas, and hepatocellular carcinomas.

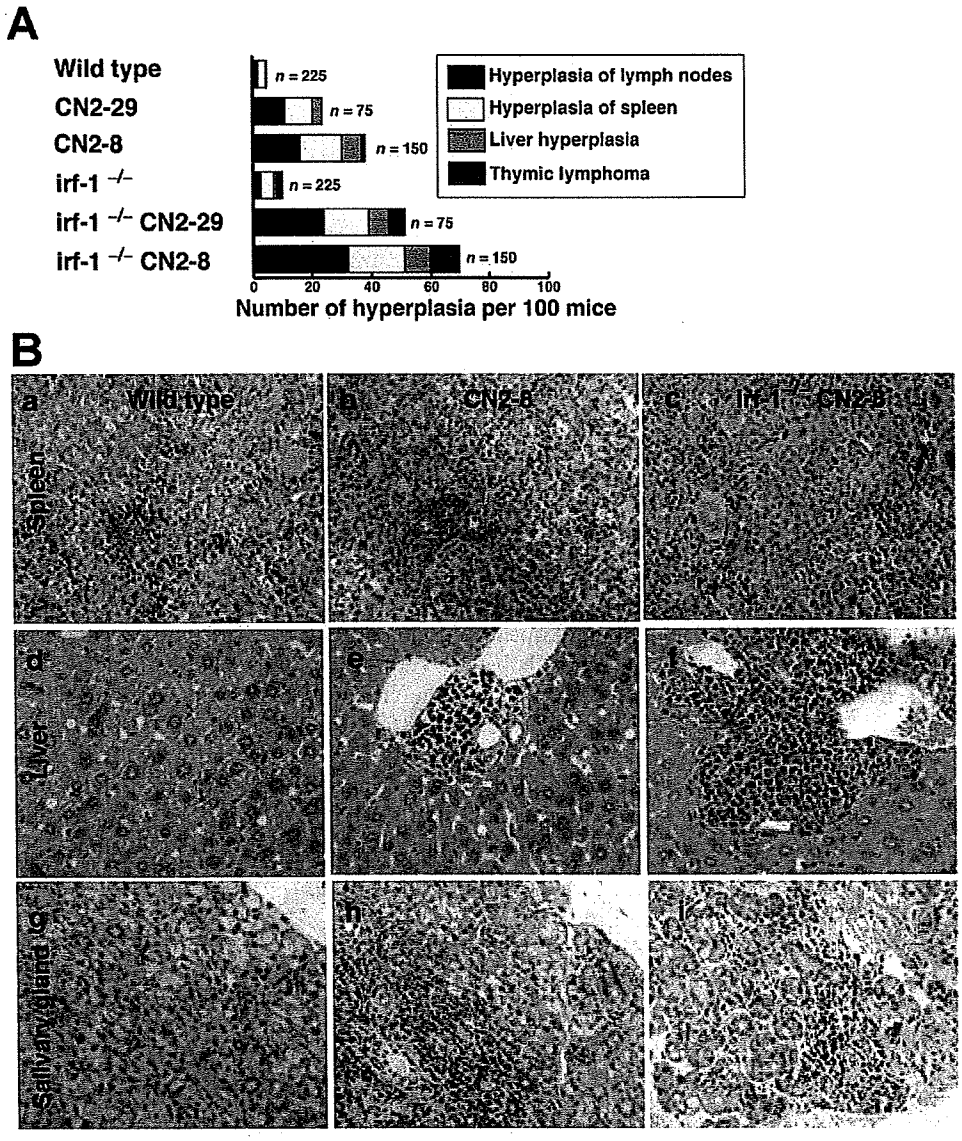

Figure 2. Disruption of *irf-1* aggravates lymphocyte infiltration in combination with HCV transgene expression. (*A*) Histologic analysis of spontaneous proliferative disturbances in the CN2 transgenic mice. Of the 900 mice injected with AxCANCre, 25 of 75 (33%) CN2-29, 47 of 150 (31%) CN2-8, 29 of 75 (39%) *irf-1*$^{-/-}$ CN2-29, and 62 of 150 (41%) *irf-1*$^{-/-}$ CN2-8 mice developed proliferative disturbances. Data shown are from the same cohort of mice analyzed in Figure 1*F*. (*B*) H&E-stained tissue sections of (*a–c*) spleens, (*d–f*) livers, and (*g–i*) salivary glands from age-matched WT, CN2, and *irf-1*$^{-/-}$ CN2 mice after the administration of AxCANCre.

mouse were significantly increased by the ablation of *irf-1* (Figure 1*F*). Although the type of hyperplasia did not differ significantly between the *irf-1*$^{-/-}$ CN2 mice and their *irf-1*$^{+/+}$ CN2 siblings, the time to onset of tumorigenesis differed dramatically (Figure 1*D* and 1*F*), indicating that age is a significant factor in the promotion of lymphomagenesis by HCV proteins.

A significant percentage of the mice that expressed the HCV core protein (*irf-1*$^{-/-}$ CN2 mice) developed polyclonal lymphoid growth disturbances, including splenomegaly, expanded lymph nodes, adenocarcinoma in the abdomen or leg, and lymphoma of the liver or Peyer's patches (Figure 2*A*). In contrast, hepatocytes with abundant expression of HCV proteins rarely developed into hepatocellular carcinomas. H&E staining of splenomegalic tissue revealed extensive hyperplasia of the white pulp zones, in which the cortical zones contained lymphoid follicles and scattered germinal centers, although mitotic figures were rarely observed (Figure 2*B* and data not shown). These results indicate that persistent expression of HCV proteins frequently induces lymphoproliferative disorders in addition to liver hyperplasia, which is consistent with the phenotype of patients with hepatocellular carcinoma.[3,4,9]

Abnormal T-Cell and B-Cell Proliferation in HCV Transgenic Mice

To characterize the disruption of lymphocyte proliferation due to HCV protein expression in the transgenic mice, we used flow cytometry to determine the ratio of T cells to B cells by staining with antibodies directed against CD3, CD45R, CD4, CD8, and the T-cell receptor. The average ratio of T cells to B cells in the lymph nodes and spleens of CN2 mice was significantly higher than

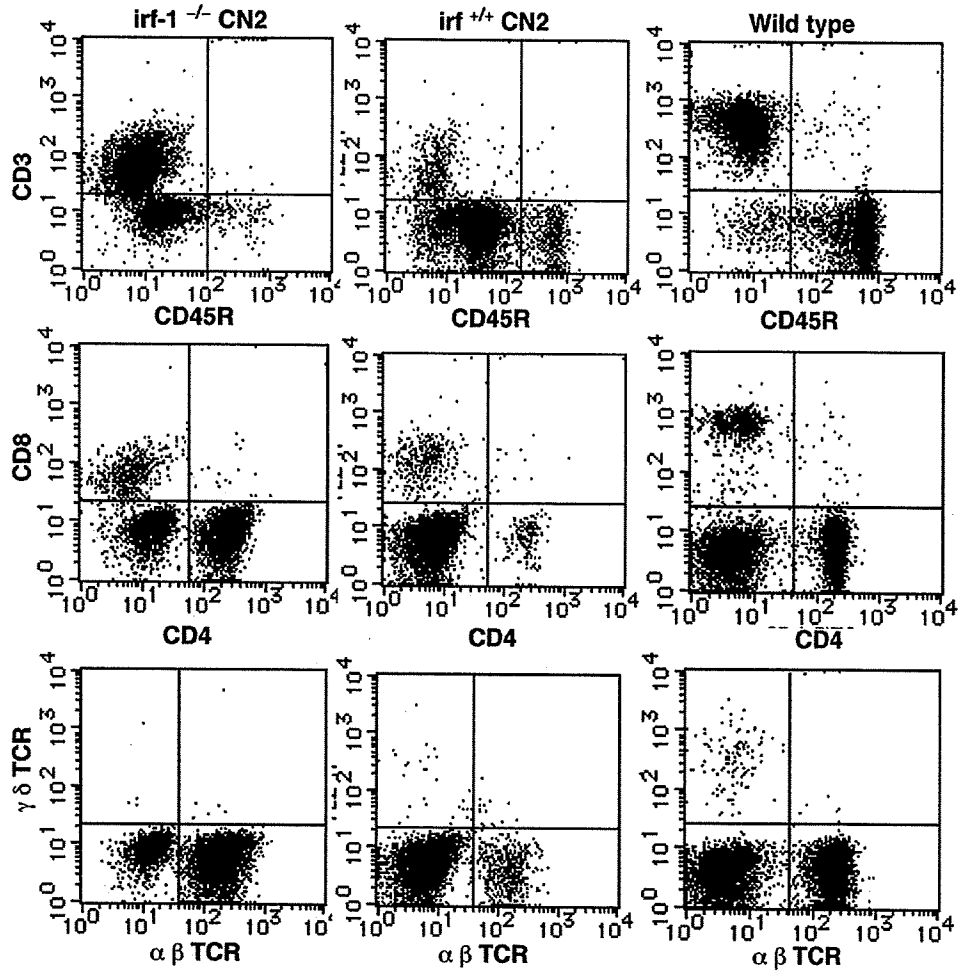

Figure 3. HCV expression and *irf-1* ablation affect the lymphocyte population. T-cell and B-cell proliferation in *irf-1*$^{+/+}$ CN2 mice, *irf-1*$^{-/-}$ CN2 mice, and WT mice. CD3$^+$, CD45R$^+$, CD4$^+$, CD8$^+$, and T-cell receptor–positive cells from age-matched *irf-1*$^{-/-}$ CN2, *irf-1*$^{+/+}$ CN2, and WT mice with hyperplasia were analyzed by fluorescence-activated cell sorting. Lymphocytes were prepared from CN2-8 and WT littermates at the age of 16 months, after administration of AxCANCre for 400 days.

that in the WT mice. The majority of the CD3$^+$ lymphocytes and a few CD8$^+$ lymphocytes expressed CD4 on their surfaces. The proliferating cells were mainly CD4$^+$ T cells, although some were CD45R$^+$B cells (Figure 3 and data not shown). The *irf-1*$^{-/-}$ CN2 mice also developed B-cell lymphomas (data not shown). These results confirm that HCV protein expression induces lymphoproliferative disorders that involve excessive expansion of both T and B cells. In *irf-1*$^{-/-}$ CN2 mice, the cell population that was negative for T-cell receptor (α, β, γ, and δ isoforms) staining was smaller than that in the other mice.

Inhibition of Fas-Induced Apoptosis Owing to Disruption of irf-1 *Leads to Persistent Expression of HCV in Transgenic Mouse Livers*

The Fas ligand is essential for the development of hepatitis via cytotoxic T-lymphocyte–mediated cell killing.[22] Therefore, we determined the sensitivities of *irf-1*$^{-/-}$ hepatocytes to Fas-induced apoptosis. The *irf-1*$^{-/-}$ mice and WT littermates were injected intravenously with a monoclonal antibody against Fas. The disruption of *irf-1* inhibited Fas-induced apoptosis, presumably by decreasing the levels of caspase-6 and -7 messenger RNA (mRNA; Supplementary Figure 2). These results suggest that the reduced expression of effector caspases delays Fas-mediated apoptosis in *irf-1*$^{-/-}$ mice and abrogates the elimination of HCV-expressing cells in vivo.

Stable Expression of HCV Proteins Induces Lymphoproliferative Diseases

To confirm that HCV proteins induce lymphoproliferation without the adenoviral vector system, switching of the expression of HCV proteins was conducted using the Mx promoter–driven cre recombinase with poly(I:C) induction (Figure 4*A*). The Mx promoter is active in hepatocytes as well as in hematopoietic cells. We crossed CN2 mice with Mx1-Cre transgenic mice; CRE recombinase was expressed from the IFN-inducible *Mx1* promoter. Injection of the Mx1-Cre/CN2-29 mice with poly (I:C) induced IFN production and efficiently induced the generation of CN2 gene products in hematopoietic cells

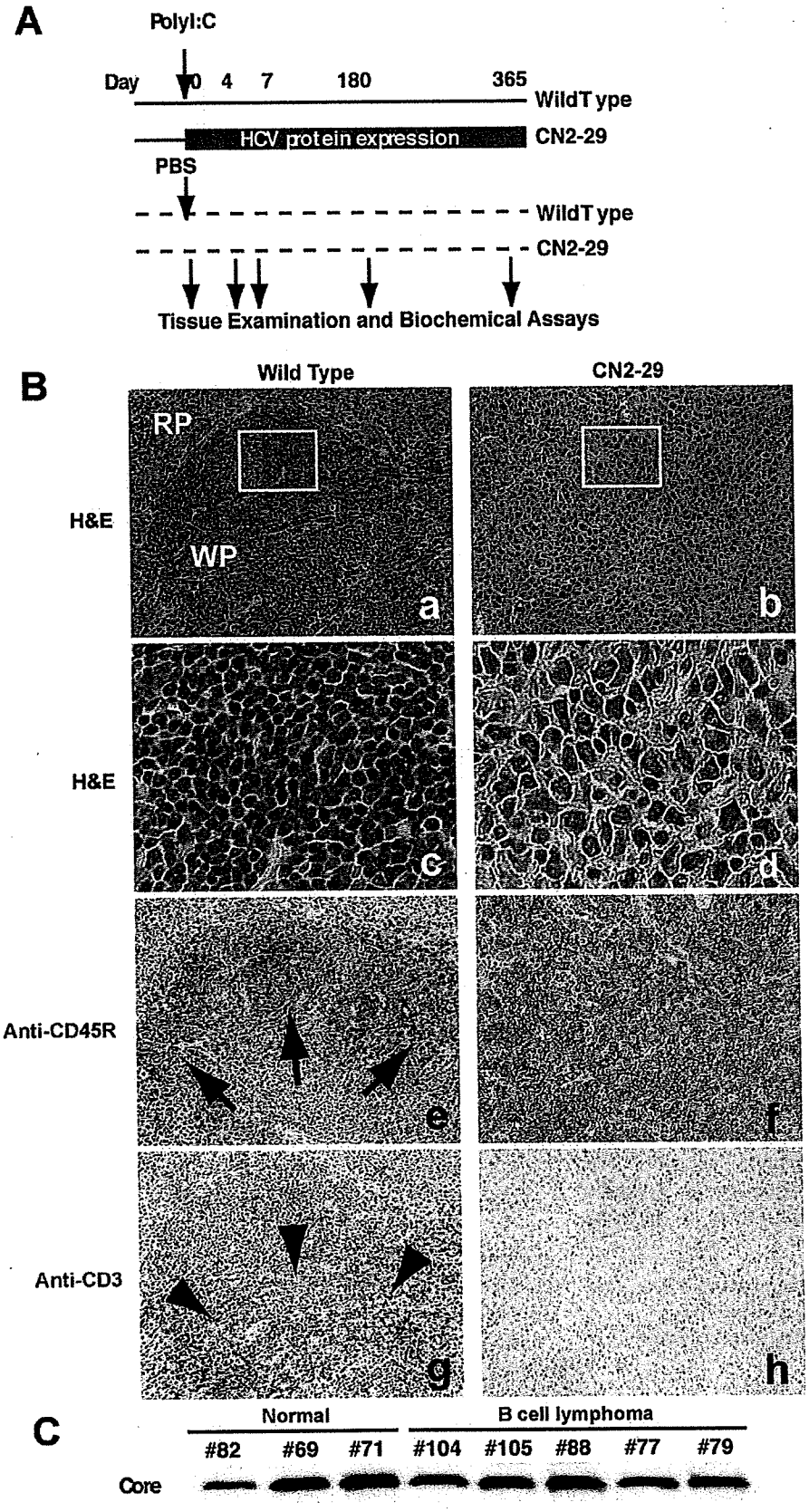

Figure 4. Stable expression of HCV viral proteins induces lymphoproliferative diseases. (*A*) Switching of the expression of HCV proteins was conducted using the Mx promoter–driven cre recombinase with poly(I:C) induction. The Mx promoter is active in hepatocytes as well as in hematopoietic cells. We crossed CN2 mice with Mx1-Cre transgenic mice; Cre recombinase was expressed from the IFN-inducible *Mx1* promoter. Injection of Mx1-Cre/CN2-29 mice with poly(I:C) induces IFN production and efficiently induces the expression of CN2 gene products in hematopoietic cells (mainly in Kupffer cells and lymphocytes), livers, and spleens but not in most other tissues. (*B*) The white pulp (WP) and red pulp (RP) comprise the components of the spleen in WT mice. The neoplastic cells replace the normal structures, such as the white pulp and red pulp. (*c* and *d*) The neoplastic cells are larger than lymphocytes (*c*), and the nuclei are irregular, round, oval, elongated, and polygonal (*d*). (*e* and *g*) The white pulp in WT mice consists of both a B-cell–rich area (*arrows*, *e*) and T-cell–rich area (*arrowheads*, *g*). (*f* and *h*) The neoplastic cells show staining for the B-cell marker CD45R, thereby supporting the diagnosis of B-cell lymphoma (*f*), while they do not show staining for the T-cell marker CD3 (*h*). *Frames c* and *d* are higher-magnification views of the white box areas in *a* and *b*, respectively. (*C*) Core protein expression was confirmed by immunoblotting.

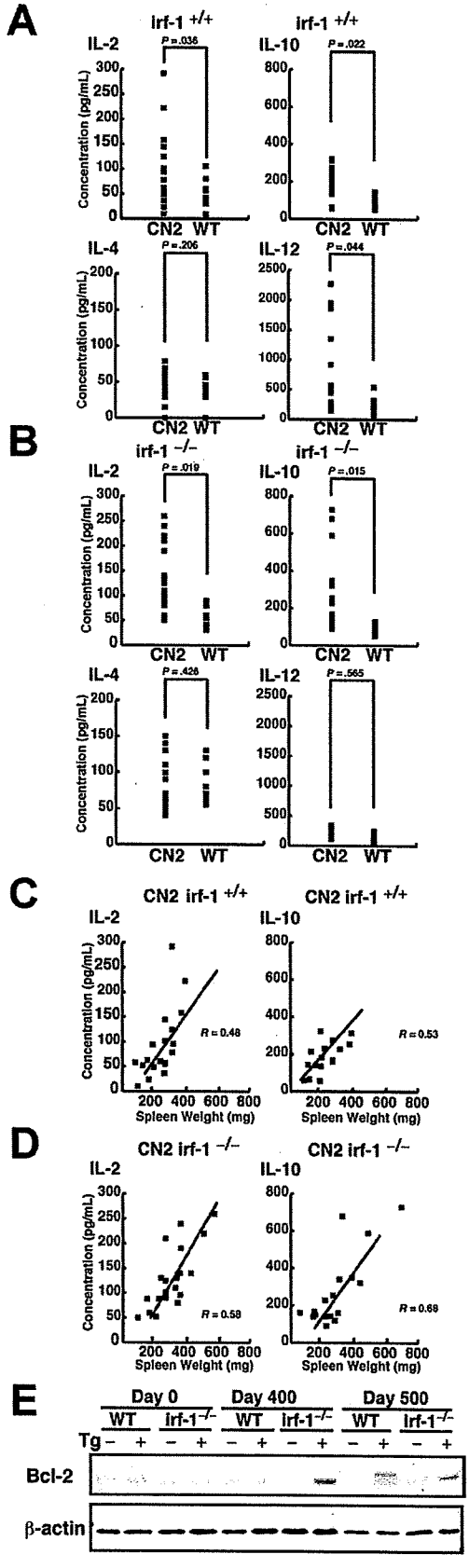

(mainly in Kupffer cells and lymphocytes), liver, and spleen but not in most other tissues. At 7 days after induction of viral proteins, HCV core proteins were detected in both hepatocytes and hematopoietic cells (data not shown). After 180 days, almost 40% of the CN2(-29) mice developed lymphomas, whereas the WT mice did not (Figure 4*B*). The neoplastic cells were larger than lymphocytes, and their nuclei were irregular, round, oval, elongated, and polygonal. HCV core protein expression was confirmed by immunoblotting (Figure 4*C*), and increases in the levels of interleukin (IL)-2, IL-10, and IL-12 were observed (data not shown). The hematopoietic marker CD45R was detected in the lymphoproliferative regions and spleens (Figure 4*B*). The efficiency of expression switching was confirmed by both the HCV transgene copy numbers and protein expression using quantitative PCR and immunoblotting, respectively (Supplementary Figure 3). These results further validate that sustained expression of HCV proteins induces lymphoproliferation.

Increased IL-2, IL-10, and IL-12 Levels in HCV Transgenic Mice

To study the mechanisms of HCV-induced lymphoproliferative diseases, we measured the serum IL-2, IL-4, IL-10, and IL-12 levels in the CN2 transgenic mice and their WT littermates (Figure 5*A*). The serum IL-4 concentration did not differ significantly between the CN2 and WT mice following injection with AxCANCre. However, the CN2 mice had significantly increased levels of serum IL-2, IL-10, and IL-12. Notably, the CN2 mice with proliferative disturbances in the lymph nodes and spleen had dramatically elevated levels of these cytokines, suggesting that altered cytokine production is involved in aberrant lymphocyte proliferation or differentiation in CN2 mice. In contrast, the *irf-1*$^{-/-}$ CN2 mice did not show elevated levels of serum IL-12 but had significantly higher levels of serum IL-2 and IL-10 compared with *irf-1*$^{-/-}$ mice (Figure 5*B*). Thus, the disruption of *irf-1* abrogates the increase in IL-12 level but augments the increases in the levels of IL-2 and IL-10 in CN2 mice. These results indicate that IL-2 and IL-10 play key roles

Figure 5. HCV protein expression alters the cytokine profile. (*A*) The serum IL-2, IL-4, IL-10, and IL-12 levels in *irf-1*$^{+/+}$ CN2 (Tg+) and *irf-1*$^{+/+}$ WT mice were measured by enzyme-linked immunosorbent assay. (*B*) The serum IL-2, IL-4, IL-10, and IL-12 levels in *irf-1*$^{-/-}$ CN2 (Tg+) and *irf-1*$^{-/-}$ WT mice were measured by enzyme-linked immunosorbent assay. The *P* values are based on comparisons of the mean cytokine concentrations. (*C* and *D*) Relationship between the IL-2 or IL-10 concentration in the serum and the spleen weights of (*C*) CN2irf-1$^{+/+}$ or (*D*) CN2irf1$^{-/-}$ mice with progressive lymphoproliferation. The numbers of points in the graphs correspond to the numbers of tested animals. (*E*) Bcl-2 protein levels in the lymph nodes of *irf-1*$^{+/+}$ (WT) and *irf-1*$^{-/-}$ transgenic (CN2) (Tg+) and WT mice on days 0, 400, and 500 after the administration of AxCANCre. Bcl-2 migrates at 26 kilodaltons. β-Actin was used as a loading control.

in the induction of the lymphoproliferative phenotype in *irf-1*$^{-/-}$ CN2 mice.

To verify the relationship between the weights of the lymph organs and the cytokine levels, the correlation coefficients were calculated according to Pearson (Figure 5*C* and 5*D*). Whereas spleen weight did not markedly influence the increase in IL-4 level (data not shown), a significant positive correlation was found between spleen weight and increased IL-2 and IL-10 levels in CN2 gene-expressing mice on the *irf-1*$^{-/-}$ background ($R = 0.58$, $P < .05$, and $R = 0.68$, $P < .05$, respectively) (Figure 5*D*). With respect to the serum levels of IL-2 and IL-10, a less intensive but significant positive correlation was found between the cytokine levels and spleen weights of CN2 gene-expressing mice on the *irf-1*$^{+/+}$ background ($R = 0.43$, $P < .05$, and $R = 0.53$, $P < .05$, respectively) (Figure 5*C*). These results indicate that IL-2 and IL-10 are involved in lymphoproliferation in viral protein-expressing mice.

Aberrant Expression of Bcl-2 in Expanded Lymph Nodes of CN2 Mice

Bcl-2 immunoglobulin transgenic mice develop follicular lymphoproliferation[23] due to the inability of various stimuli to induce apoptosis in these mice.[24] Therefore, to examine whether HCV causes dysregulation of Bcl-2 in lymphoid tissues, we examined the expression of Bcl-2 (Figure 5*E*). Lymph nodes collected from *irf-1*$^{-/-}$ CN2 mice 400 days after the administration of AxCANCre showed elevated levels of Bcl-2. Immunoblot analysis revealed that a doublet for Bcl-2 (26 and 28 kilodaltons) appeared in some samples 500 days after AxCANCre administration, suggesting the presence of phosphorylated and nonphosphorylated Bcl-2.[25]

Combination Cytokine Treatment Enhances Splenocyte Colony Formation in Synergy With Viral Protein Expression

To determine whether aberrant cytokine profiles contribute to lymphocyte transformation, a colony formation assay was performed using the methylcellulose method. Mouse splenocytes were infected with adenoviruses that expressed the *cre* DNA recombinase or *lacZ* control. Expression of HCV core proteins was induced by cre-adenovirus infection of the splenocytes (Figure 6*A*). Colony counting was performed at postinfection day 28 (Figure 6*B*). Combined treatment with IL-2 and IL-10 greatly enhanced colony formation, especially in the splenocytes of HCV transgenic mice (CN2-29, *irf-1*$^{-/-}$ CN2-29). The addition of IL-12 suppressed colony formation induced by combined treatment with IL-2 and IL-10. In the *irf-1*$^{-/-}$ background, treatment with IL-2 plus IL-10 or IL-2 plus IL-12 greatly enhanced colony formation. To determine whether enhanced colony formation correlated with cytokine-induced Bcl-2 expression, the Bcl-2 mRNA levels in the splenocytes were quantified (Figure 6*C*). Because IL-2 enhances T-lymphocyte proliferation and transformation,[26] it is of particular interest that treatment with IL-2 plus IL-10 resulted in marked increases in both lymphocyte transformation and the Bcl-2 mRNA levels upon HCV transgene expression. These results indicate that dysregulated cytokine expression, disruption of *irf-1*, and HCV transgene expression synergistically enhance splenocyte transformation.

Cytokine Treatment and HCV Transgene Expression Synergistically Inhibit Fas-Mediated Apoptosis

To determine whether cytokines inhibit Fas-induced apoptosis, we treated the splenocytes from transgenic and WT mice with cytokines and then measured Fas-induced apoptosis by Annexin V staining and fluorescence-activated cell sorting, and we also assayed caspase enzymatic activity (Figure 6*D* and 6*E*). IL-10 treatment in the presence of IL-2 greatly inhibited Fas-induced apoptosis. Furthermore, *irf-1* disruption made the splenocytes resistant to Fas-induced apoptosis in the presence of IL-2, IL-10, and/or IL-12. In particular, IL-2 plus IL-10 treatment produced the strongest inhibition of Fas-induced apoptosis. These cytokines also up-regulated the Bcl-2 mRNA levels in splenocytes, which indicates that IL-2, IL-10, and/or IL-12 up-regulate *bcl-2* expression, which subsequently inhibits Fas-induced apoptosis. This result is consistent with reports that IL-10 and/or IL-2 treatment induce *bcl-2* in B or T lymphocytes.[10,27] Caspase-3/7 activity was correlated with the level of *bcl-2* expression (Figure 6*C* and 6*F*). These results indicate that aberrant cytokine expression and disruption of IFN signaling affect *bcl-2* expression, which is associated with the inhibition of caspase expression.

HCV Core and E2 Proteins Mediate IL-2, IL-10, and IL-12 Expression

To determine which viral protein is responsible for cytokine expression, individual viral proteins were stably expressed in splenocytes using recombinant lentiviruses that express the HCV core, E1, E2, NS2, and lacZ. Each gene expression profile was confirmed by reverse-transcription PCR (Supplementary Figure 4). Only the HCV core protein induced IL-2 and IL-10 (Figure 7*A*). To determine whether extracellular viral proteins trigger cytokine expression, recombinant viral proteins were added to the cells. Only the viral envelope protein E2 induced IL-12 (Figure 7*B*). These results indicate that the HCV core and E2 proteins are responsible for IL-2, IL-10, and IL-12 expression.

HCV Core and IL-10 Induce Bcl-2 Expression

To determine whether viral protein expression and cytokine stimulation synergistically induce Bcl-2 expression, individual viral proteins were stably expressed using lentiviral vectors, and the cells were tested for Bcl-2 expression. Core protein expression and IL-10 stimula-

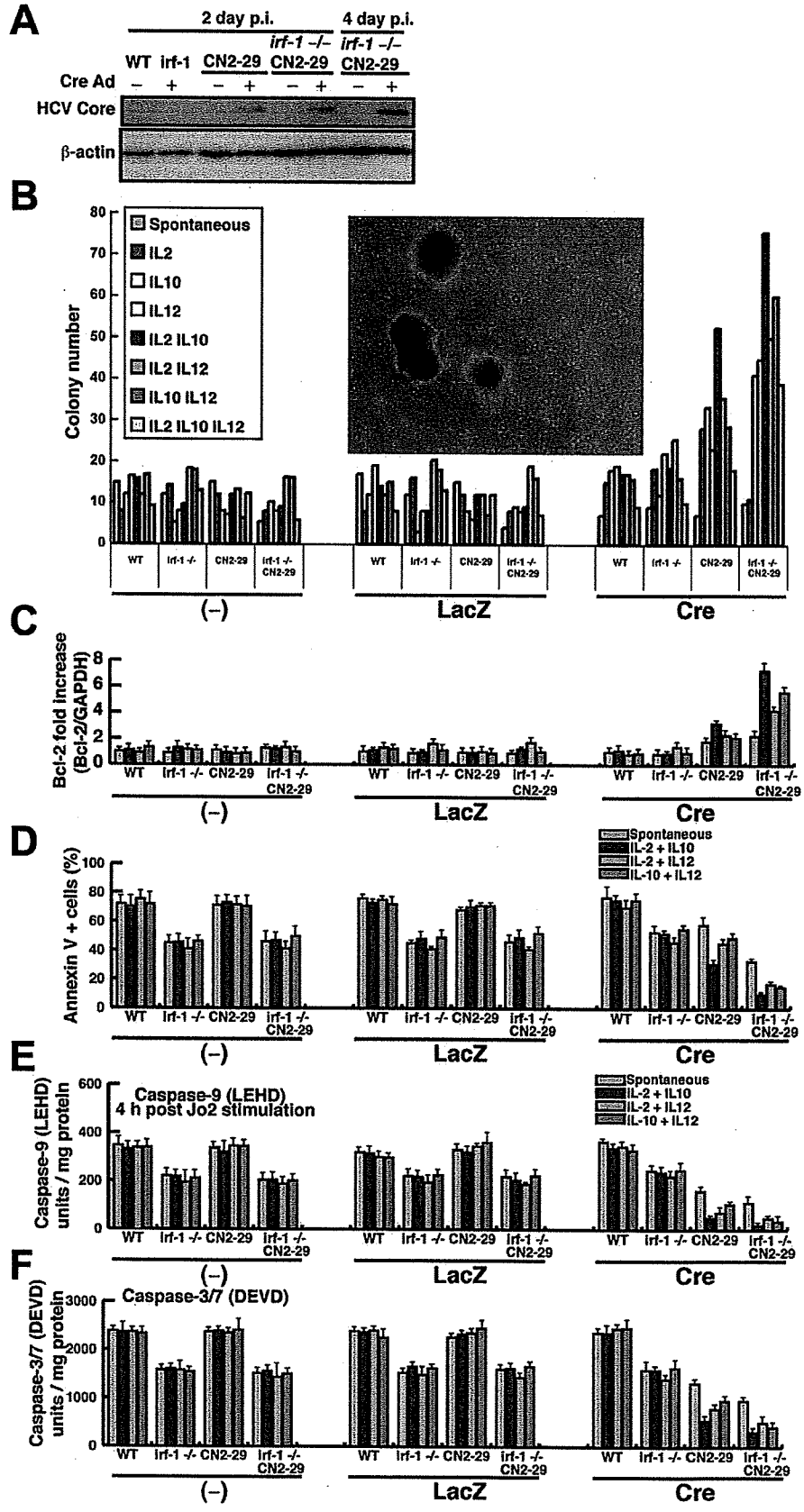

Figure 6. Lymphocyte transformation by aberrant cytokines and inhibition of apoptotic signaling. (*A*) Expression of the HCV core protein (21 kilodaltons) in *irf-1*$^{+/+}$ (WT) and *irf-1*$^{-/-}$ transgenic (CN2-29) and WT mice 2 or 4 days postinfection (p.i.) with AxCANCre (multiplicity of infection, 1.0). β-Actin was used as a loading control. (*B*) Colony formation assay for splenocytes from *irf-1*$^{+/+}$ (WT) and *irf-1*$^{-/-}$ WT or transgenic (CN2-29) mice in the absence or presence of the indicated cytokine and infected with mock, LacZ, and Cre adenoviruses. The *inset* shows an image of the colonies generated from the *irf-1*$^{-/-}$ CN2 splenocytes (original magnification 10×). (*C*) Quantification, by quantitative reverse-transcription PCR of Bcl-2 mRNA relative to control glyceraldehyde-3-phosphate dehydrogenase mRNA in the splenocytes of *irf-1*$^{+/+}$ (WT) and *irf-1*$^{-/-}$ or transgenic (CN2-29) mice treated with the indicated cytokines and infected with mock, LacZ, and cre adenoviruses. (*D*) Apoptosis measured by Annexin V fluorescence-activated cell sorting analysis of splenocytes from *irf-1*$^{+/+}$ (WT) and *irf-1*$^{-/-}$ or transgenic (CN2-29) mice treated with the indicated cytokines and infected with the mock, LacZ, and cre adenoviruses. (*E* and *F*) The caspase-9 and caspase-3/7 enzymatic activities in splenocytes from *irf-1*$^{+/+}$ (WT) and *irf-1*$^{-/-}$ or transgenic (CN2-29) mice treated with the indicated cytokines were measured using a substrate cleavage assay after infection with the mock, LacZ, and Cre adenoviruses. Caspase-9 activity was measured 4 hours after injection of the anti-Fas monoclonal antibody (Jo2). LEHD, substrate for caspase-9; DEVD, substrate for caspase-3/7. Vertical bars are SD and were determined using the Student *t* test.

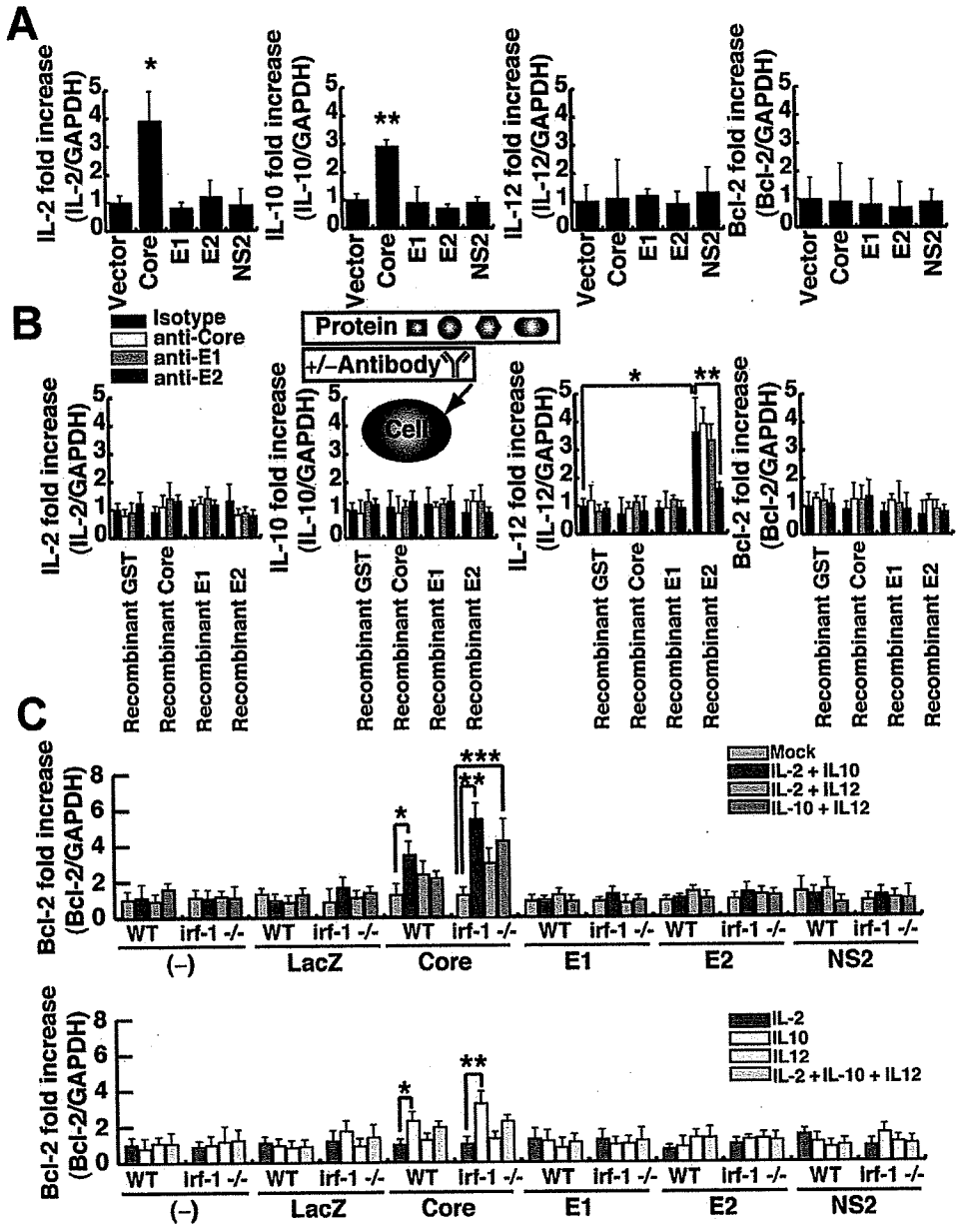

Figure 7. Induction of IL-2 and IL-10 by HCV core and IL-12 by E2 and of Bcl-2 by HCV core plus cytokines. (*A*) Individual viral proteins were stably expressed in splenocytes using recombinant lentiviruses that expressed the HCV core, E1, E2, NS2, and lacZ. Each gene expression profile was determined by quantitative reverse-transcription PCR. (*B*) E2 binding induces IL-12 in Raji cells, as determined by quantitative reverse-transcription PCR. Cells were treated with HCV core, E1, E2 (genotypes 1a and 1b), or glutathione *S*-transferase proteins, and the cytokine and bcl2 cellular RNA levels were examined using quantitative reverse-transcription PCR. (*C*) Quantification by quantitative reverse-transcription PCR of Bcl-2 mRNA relative to control glyceraldehyde-3-phosphate dehydrogenase mRNAin splenocytes from *irf-1*$^{+/+}$ (WT) and *irf-1*$^{-/-}$ WT or irf-1$^{-/-}$ mice treated with the indicated cytokines and infected with lentiviruses that express mock, core, E1, E2, NS2, and LacZ. Individual viral proteins were stably expressed using lentiviral vectors, and the cells were tested for Bcl-2 expression.

tion induced Bcl-2, while the other proteins did not (Figure 7C). Interestingly, the combination of IL-2 and IL-12 only induced Bcl-2 in the *irf-1*$^{-/-}$ background, while triple stimulation (IL-2, IL-10, and IL-12) did not induce Bcl-2 (Figure 7C). These results indicate that complex signaling networks induce Bcl-2 in the presence of viral nucleocapsid proteins.

Discussion

The present study shows that Bcl-2 levels, cytokine levels, aging, and inflammation enhance the development of lymphoproliferative disorders caused by HCV proteins (Supplementary Figure 5). Disruption of *irf-1* enables the persistent expression of HCV protein, leading to lymphoproliferative diseases owing to reduced apoptosis (ie, lower levels of caspase-1, -6, and -7 expression). HCV CN2 transgenic (Tg+) mice are resistant to Fas-induced apoptosis due to the inhibition of cytochrome *c* release from mitochondria.[16] Mice with disruption of *irf-1* have several defects of their innate and adaptive immunity, such as lineage-specific defects in thymocyte development; immature T cells can develop into mature CD4$^+$ cells but not into CD8$^+$ T cells.[18,28] IRF-1 controls the positive and negative selection of CD8$^+$ thymocytes.[29] IRF-1 is required for the development of the Th1-type immune response, and

its absence leads to the induction of the Th2-type immune response.[18,30] Because the number of natural killer cells is dramatically reduced in *irf-1*$^{-/-}$ mice,[18] this defect may cause the marked increase in viral protein expression and the inhibition of tumor surveillance mechanisms, leading to the development of non-Hodgkin's lymphoma. Expression of the IL-12 p40 subunit is defective in *irf-1*$^{-/-}$ mice.[18]

Lymphomagenesis may require the additional genetic instability provided by HCV-induced hypermutation (2-hit model). Important questions are raised regarding the lymphoproliferative mechanisms of lymphomas in HCV-infected patients (B-cell malignancies predominate). Hypermutation of the immunoglobulin genes in B cells induced by HCV infection is the cause of the lymphomagenesis seen in HCV infection,[21,31] and this model may provide more direct insights into lymphoma production, because HCV-induced hypermutation causes genetic instability and causes chromosomal aberrations, possibly resulting in neoplastic transformation.[32] In addition, the antiapoptotic phenotype generated by sustained viral protein expression may enhance the survival of lymphocytes and inhibit activation-induced cell death to turn off the activated lymphocytes. The dysregulated cytokine profiles and sustained lymphocyte survival may alter the fates of regulatory T cells and dendritic cells.[33]

In conclusion, the present study shows that the conditional expression of HCV proteins induces inflammation and lymphoproliferative disorders, which are enhanced by *irf-1* disruption. Therefore, IRF-1–inducible genes probably play essential roles in suppressing HCV-induced lymphoma and in eliminating HCV protein-expressing cells. Our transgenic mice provide evidence that the overexpression of apoptosis-related proteins, including Bcl-2, and/or aberrant cytokine production are primary events in HCV-induced lymphoproliferation. It is interesting to note that lymphoproliferation was dominant over liver tumor development in the present study. Approximately 40% of the CN2-29Mx1Cre mice developed B-cell lymphomas, while 5% of the mice developed liver tumors. Further molecular analyses will enlighten the differential signaling pathways between hepatocytes and lymphocytes and increase our understanding of the differences between lymphomagenesis and liver tumor development caused by HCV.

Supplementary Data

Note: To access the supplementary material accompanying this article, visit the online version of *Gastroenterology* at www.gastrojournal.org, and at doi: 10.1053/j.gastro.2009.03.061.

References

1. Saito I, Miyamura T, Ohbayashi A, et al. Hepatitis C virus infection is associated with the development of hepatocellular carcinoma. Proc Natl Acad Sci U S A 1990;87:6547–6549.
2. Simonetti RG, Camma C, Fiorello F, et al. Hepatitis C virus infection as a risk factor for hepatocellular carcinoma in patients with cirrhosis. A case-control study. Ann Intern Med 1992;116: 97–102.
3. Ferri C, Monti M, La Civita L, et al. Infection of peripheral blood mononuclear cells by hepatitis C virus in mixed cryoglobulinemia. Blood 1993;82:3701–3704.
4. Silvestri F, Pipan C, Barillari G, et al. Prevalence of hepatitis C virus infection in patients with lymphoproliferative disorders. Blood 1996;87:4296–4301.
5. Rui L, Goodnow CC. Lymphoma and the control of B cell growth and differentiation. Curr Mol Med 2006;6:291–308.
6. Dietrich CF, Lee JH, Herrmann G, et al. Enlargement of perihepatic lymph nodes in relation to liver histology and viremia in patients with chronic hepatitis C. Hepatology 1997;26:467–472.
7. Ascoli V, Lo Coco F, Artini M, et al. Extranodal lymphomas associated with hepatitis C virus infection. Am J Clin Pathol 1998; 109:600–609.
8. De Vita S, De Re V, Sansonno D, et al. Gastric mucosa as an additional extrahepatic localization of hepatitis C virus: viral detection in gastric low-grade lymphoma associated with autoimmune disease and in chronic gastritis. Hepatology 2000;31: 182–189.
9. Mele A, Pulsoni A, Bianco E, et al. Hepatitis C virus and B-cell non-Hodgkin lymphomas: an Italian multicenter case-control study. Blood 2003;102:996–999.
10. Cohen SB, Crawley JB, Kahan MC, et al. Interleukin-10 rescues T cells from apoptotic cell death: association with an upregulation of Bcl-2. Immunology 1997;92:1–5.
11. Pawlotsky JM. The nature of interferon-alpha resistance in hepatitis C virus infection. Curr Opin Infect Dis 2003;16:587–592.
12. Levine AM, Shimodaira S, Lai MM. Treatment of HCV-related mantle-cell lymphoma with ribavirin and pegylated interferon alfa. N Engl J Med 2003;349:2078–2079.
13. Moriya K, Fujie H, Shintani Y, et al. The core protein of hepatitis C virus induces hepatocellular carcinoma in transgenic mice. Nat Med 1998;4:1065–1067.
14. Lerat H, Honda M, Beard MR, et al. Steatosis and liver cancer in transgenic mice expressing the structural and nonstructural proteins of hepatitis C virus. Gastroenterology 2002;122:352–365.
15. Wakita T, Taya C, Katsume A, et al. Efficient conditional transgene expression in hepatitis C virus cDNA transgenic mice mediated by the Cre/loxP system. J Biol Chem 1998;273:9001–9006.
16. Machida K, Tsukiyama-Kohara K, Seike E, et al. Inhibition of cytochrome c release in Fas-mediated signaling pathway in transgenic mice induced to express hepatitis C viral proteins. J Biol Chem 2001;276:12140–12146.
17. Yokota T, Oritani K, Takahashi I, et al. Adiponectin, a new member of the family of soluble defense collagens, negatively regulates the growth of myelomonocytic progenitors and the functions of macrophages. Blood 2000;96:1723–1732.
18. Taki S, Sato T, Ogasawara K, et al. Multistage regulation of Th1-type immune responses by the transcription factor IRF-1. Immunity 1997;6:673–679.
19. Yanagi M, Purcell RH, Emerson SU, et al. Transcripts from a single full-length cDNA clone of hepatitis C virus are infectious when directly transfected into the liver of a chimpanzee. Proc Natl Acad Sci U S A 1997;94:8738–8743.
20. Yanagi M, St Claire M, Shapiro M, et al. Transcripts of a chimeric cDNA clone of hepatitis C virus genotype 1b are infectious in vivo. Virology 1998;244:161–172.
21. Machida K, Cheng KT, Pavio N, et al. Hepatitis C virus E2-CD81 interaction induces hypermutation of the immunoglobulin gene in B cells. J Virol 2005;79:8079–8089.

22. Kondo Y, Sung VM, Machida K, et al. Hepatitis C virus infects T cells and affects interferon-gamma signaling in T cell lines. Virology 2007;361:161–173.
23. McDonnell TJ, Deane N, Platt FM, et al. bcl-2-immunoglobulin transgenic mice demonstrate extended B cell survival and follicular lymphoproliferation. Cell 1989;57:79–88.
24. Lacronique V, Mignon A, Fabre M, et al. Bcl-2 protects from lethal hepatic apoptosis induced by an anti-Fas antibody in mice. Nat Med 1996;2:80–86.
25. Ito T, Deng X, Carr B, et al. Bcl-2 phosphorylation required for anti-apoptosis function. J Biol Chem 1997;272:11671–11673.
26. Stern JB, Smith KA. Interleukin-2 induction of T-cell G1 progression and c-myb expression. Science 1986;233:203–206.
27. Levy Y, Brouet JC. Interleukin-10 prevents spontaneous death of germinal center B cells by induction of the bcl-2 protein. J Clin Invest 1994;93:424–428.
28. Taniguchi T, Ogasawara K, Takaoka A, et al. IRF family of transcription factors as regulators of host defense. Annu Rev Immunol 2001;19:623–655.
29. Penninger JM, Sirard C, Mittrucker HW, et al. The interferon regulatory transcription factor IRF-1 controls positive and negative selection of CD8+ thymocytes. Immunity 1997;7:243–254.
30. Lohoff M, Ferrick D, Mittrucker HW, et al. Interferon regulatory factor-1 is required for a T helper 1 immune response in vivo. Immunity 1997;6:681–689.
31. Machida K, Cheng KT, Sung VM, et al. Hepatitis C virus induces a mutator phenotype: enhanced mutations of immunoglobulin and protooncogenes. Proc Natl Acad Sci U S A 2004;101:4262–4267.
32. Machida K, Kondo Y, Huang JY, et al. Hepatitis C virus (HCV)-induced immunoglobulin hypermutation reduces the affinity and neutralizing activities of antibodies against HCV envelope protein. J Virol 2008;82:6711–6720.
33. Dolganiuc A, Paek E, Kodys K, et al. Myeloid dendritic cells of patients with chronic HCV infection induce proliferation of regulatory T lymphocytes. Gastroenterology 2008;135:2119–2127.

Received June 25, 2008. Accepted March 31, 2009.

Reprint requests

Address requests for reprints to: Michinori Kohara, PhD, Department of Microbiology and Cell Biology, Tokyo Metropolitan Institute of Medical Science, 3-18-22 Honkomagome, Bunkyo-ku, Tokyo 113-8613, Japan. e-mail: mkohara@rinshoken.or.jp; fax: (81) 3-3828-8945.

Acknowledgments

The authors thank Prof Tadatsugu Taniguchi for his scholarly support of this study; Kazuaki Inoue and Kentaro Tomita for their advice on histology; Yutaka Amako, Isao Maruyama, and Kohsuke Tanaka for technical assistance; and Mitsugu Takahashi for breeding the transgenic mice.

Conflicts of interest

The authors disclose no conflicts.

Funding

Supported in part by a research fellowship from the Japan Society for the Promotion of Science; a grant from the Ministry of Education, Culture, Sports, Science and Technology of Japan; a grant from the Ministry of Health, Labour and Welfare of Japan; and the Program for Promotion of Fundamental Studies in Health Sciences of the National Institute of Biomedical Innovation of Japan. This project was also supported by National Institutes of Health research grants P50AA11999, 5P30DK048522-13, and CA108302.